Communs geol. Surv. Namibia, ***11*** *(1996), 23-31*

Scapolitization in the Kuiseb Formation of the Damara Orogen: geochemical and sTable 1sotope evidence for fluid infiltration along deep crustal shear zones

A. Dombrowski[1], S. Hoernes[2] and M. Okrusch[1]

[1]*Mineralogisches lnstitut, Universität Würzburg, Am Hubland, 97074 Würzburg, Germany*

[2]*Mineralogisch-Petrologisches lnstitut, Poppelsdorfer Schloß, 53115 Bonn, Germany*

In the Pan-African Damara Orogen, an unusual scapolitization occurs within metaturbidites of the Kuiseb Formation in the Khomas Hochland, central Namibia. Geochemical investigations exclude an evaporitic precursor for the scapolite-bearing Kuiseb schists. Carbon isotope data indicate a local sedimentary source of fluids which reacted with pre-existing plagioclase in the Kuiseb schists to form the scapolite.

Introduction

Scapolite formation in amphibolite facies meta-sedimentary rocks may be attributed to either evaporites as protoliths (Mora and Valley, 1989; Gómez-Pugnaire *et al.*, 1994; Behr *et al.*, 1983), or interaction with externally derived chlorine- and/or CO_2-rich fluids during metamor-phism (Oliver *et al.*, 1992). Deciphering an evaporitic nature for the scapolite-forming process is difficult because clear evidence such as pseudomorphs after evaporite minerals (e.g. halite) are generally lacking.

We present a case study within rocks of the Pan-African Kuiseb Formation in central Namibia where two horizons of scapolite-bearing schists are traceable for more than one hundred kilometres along strike (Kukla, P.A., 1990, 1992; Kukla, C., 1993), raising the question of whether or not this represents a possible primary sedimentary feature. Geochemical analyses of bulk rock compositions, rare earth element (REE) patterns, as well as sTable 1sotope compositions of carbon in scapolite and calcite will be used to address this question.

Geological setting

The study area is located in the northern part of the Khomas Hochland, central Namibia (Fig. 1). This part of the Pan-African Damara Orogen is made up by rocks of the Kuiseb Formation, which consists of a monotonous sequence of schistose pelitic and psammitic meta-

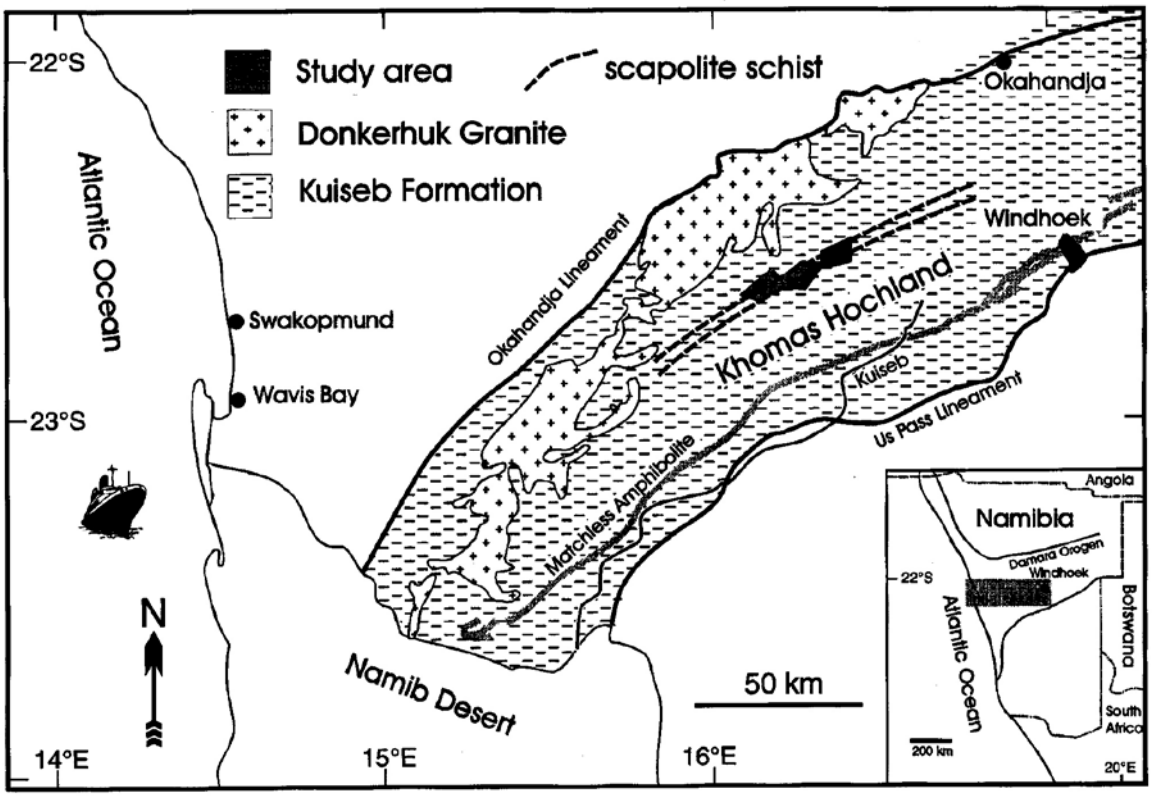

Figure 1: Map showing the location and simplified regional geological setting of the study area.

turbidites with intercalations of graphitic schist, calc-silicate rocks, marble, tremolite schist, scapolite schist and the Matchless amphibolite. Metamorphic conditions were of amphibolite facies grade with a progressive northward increase in peak temperatures reaching anatectic conditions in the northern Khomas Hochland near the syn-orogenic Donkerhoek granite (e.g. Hartmann *et al.*, 1983; Kukla, P.A., 1992; Kukla, C., 1993; Bühn *et al.*, 1994). Most textural evidence for the polyphase deformation history has been overprinted by post-tectonic growth of the minerals. For the geotectonic evolution of the Khomas Hochland, Kukla and Stanistreet (1991) established a tectono-sedimentary model comprising the evolution of an accretionary prism within a convergent continental margin setting. According to Kukla (1992), the scapolite-bearing assemblages are associated with two of the major high strain zones that subdivide the Khomas Trough in the form of structural discontinuities. Kukla (1990, 1992), therefore, interpreted scapolitization as a product of fluid movement along these zones of tectonic weakness which led to an interaction of the Kuiseb schists with saline brines either from early rift-related sequences or pore fluids which were being expelled from the accretionary prism.

Analytical procedures

Major and trace elements as well as Cl concentrations were determined from fused discs by conventional XRF methods using a Philips PW1410 spectrometer. Lithium was analysed by atomic absorption using a Perkin Elmer 300. CO_2 was determined volumetrically.

The REE contents were analysed, using the facilities of the GeoForschungsZentrum Pots dam, by ICP-AES, after decomposing the samples in HF-$HClO_4$ and separating the REE in chromatographic columns (Zuleger and Erzinger, 1988). Chondri tic normalizing factors are taken from Evenson *et al.* (1978). Subscript *N* in the text indicates chondrite normalized values.

STable 1sotope analyses were carried out at the Mineralogical Institute of the Bonn University using a Prism I by VG Instruments. The finely ground sample powders were treated with 100% H_3PO_4 at different temperatures. Reaction at 25°C for one hour was sufficient to dissolve nearly completely the usually small contents of calcite. The liberated CO_2 was collected and measured in the mass spectrometer. The small amount of gas produced during a further two hours of reaction at 25°C was pumped away. Extraction of CO_2 from the scapolite structure occurred at 75°C over at least 12 hours of reaction. The temperature was maintained by placing the reaction vessel in a dry heat box, simultaneously cooling the stopcocks by a stream of air at room temperature. To test the results of the scapolite analysis, the samples were immersed in dilute HCI to remove any calcite and then reacted with 100 % H_3PO_4 in the described manner (cf. Moecher *et al.*, 1994). The results of both methods agree within analytical error. Analytical precision for ∂-values from scapolite is in the range of ± 0.15-0.2‰. Values of $\partial^{13}C$ are reported in the standard per mil notation relative to PDB.

Figure 2: Spheroidal scapolite porphyroblasts (white) in scapolite schist of the Kuiseb Formation.

Sample description

The scapolite-bearing Kuiseb schists are characterized in the field by a dark grey colour when fresh, but their behaviour during weathering gives them a typically speckled appearance (Fig. 2). The extent of scapolitization is very variable in the investigated samples with scapolite contents of up to 60 vol. % of the rock.

The occurrence of scapolitization under static conditions is shown by the presence of large postkinematic poikiloblasts, up to several millimetres in diameter. These are of mizzonitic composition, with an average formula of $Na_{1.5}Ca_{2.5}Al_{4.6}Si_{7.4}O_{24}Cl_{0.3}(CO_3)_{0.7}$ (Table 1), and rest in a matrix of biotite and quartz with various minor phases such as epidote, calcite, Ca-amphibole and titanite. In contrast to the adjacent metaturbidites, primary sedimentary features and deformation structures are largely obliterated. The scapolite-free Kuiseb metasedimentary rocks are characterized by the equilibrium assemblage staurolite + garnet + biotite ± muscovite ± sillimanite + quartz ± plagioclase reflecting metamorphic conditions of the lower amphibolite facies, with temperatures of 550 - 650°C and pressures of 2.5-5.5 kb (Kukla, 1992; Bühn *et al.*, 1994).

Major and trace element geochemistry

Recognition of metamorphosed evaporites in metasedimentary series is difficult and relies mainly on indirect evidence, because of the major changes in mineral content and bulk rock composition possible during metamorphism. The increasing solubility of NaCl in water with increasing temperature, for example, is responsible for the complete disappearance of halite crystals during diagenesis and early stages of metamorphism. Since pseudomorphs after evaporite minerals in metamorphic rocks are scarce, former evaporites are often assumed when minerals such as scapolite, lazurite or tourmaline occur, or highly saline fluid inclusions are found. Such interpretations are, however, rarely unequivocal.

Comparison between the geochemical characteristics of evaporitic sediments and their metamorphosed equivalents is problematic since metamorphism generally leads to the removal of volatile components and changes in bulk rock chemistry are common. Moine *et al.* (1981) developed some discriminating criteria based on elements believed to be relatively inert during metamorphic processes. They found Mg, Al, Fe, Ca and Li to be the least affected elements and that these reveal characteristic differences between evaporitic and non-evaporitic sediments. The scapolite-bearing Kuiseb schists are distinctly different from (meta-) evaporitic sediments (Table 2), according to the discriminating criteria of Moine *et al.* (1981). The position of the Kuiseb schists, whether scapolite-bearing or not, in the triangular plot Ca-Mg-Al (Fig. 3) is identical to that of common platform sediments and modem turbidites, implying that derivation of these scapolite-bearing assemblages from an evaporitic precursor is unlikely. Compared to the scapolite-free Kuiseb schists, the scapolite schists are characterized by a shift towards the Ca apex of the plot. In general, a distinctly higher Ca content of the scapolite schists is the major and significant differ-

Table 1: Representative microprobe analyses of scapolite from the Kuiseb Formation.

	AD93-35	AD93-35	AD93-8	AD93-8	AD93-9	AD93-9
wt.%						
SiO_2	49.23	47.80	48.77	48.54	47.71	47.66
Al_2O_3	26.17	26.46	25.96	26.18	25.90	25.94
CaO	15.00	15.54	15.52	15.21	15.32	15.18
Na_2O	4.80	4.48	4.63	4.69	4.56	4.71
K_2O	0.78	0.62	0.71	0.80	0.49	0.51
SO_3	0.06	0.00	0.03	0.03	0.02	0.00
Cl	1.22	1.08	1.16	1.17	0.97	1.20
Total	97.26	95.98	96.78	96.62	94.97	95.20
Atomic proportions based on 12 <Si+Al>						
Si	7.38	7.26	7.37	7.34	7.32	7.31
Al	4.62	4.74	4.63	4.66	4.68	4.69
Total	12.00	12.00	12.00	12.00	12.00	12.00
Ca	2.41	2.53	2.51	2.46	2.52	2.49
Na	1.40	1.32	1.36	1.37	1.36	1.40
K	0.15	0.12	0.14	0.15	0.10	0.10
Total	3.96	3.97	4.01	3.98	3.98	3.99
%Mej[a]	61.02	63.78	62.88	61.86	63.55	62.67
Eq.An[b]	54.07	57.95	54.19	55.44	56.08	56.32

[a]= (Ca/(Ca+Na+K)) * 100 (Shaw, 1960)
[b]= 100(Al-3)/3 (Orville, 1975)
Fe, Ti, Mg and Mn are below detection limit.
The whole data set is available on request.

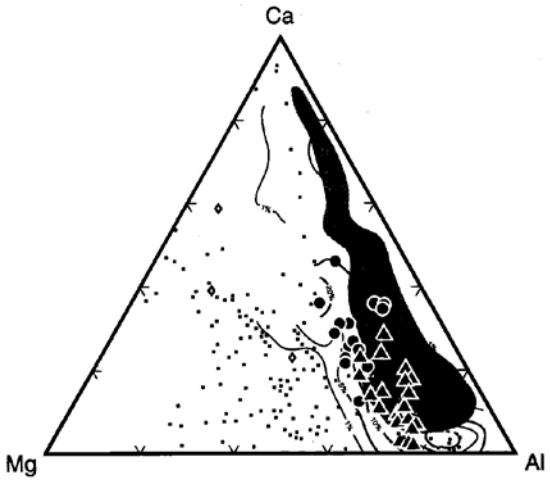

Figure 3: Triangular plot Ca-Mg-Al after Moine *et al.* (1981). Contour lines = density lines of the reference set of common platform sediments, shaded field = 69 analyses from modern turbidites from McLennan *et al.* (1990) where the darker area represents 50% of the data points; ● = scapolite-bearing schists and ▲ = scapolite-free metasedimentary rocks of the Kuiseb Formation; • = evaporites and ◊ = NaCl-bearing evaporites, from Moine *et al.* (1981; Table 2).

Table 2: Geochemical characteristics of scapolite - bearing Kuiseb schists in comparison with those of evaporites and meta-evaporites documented by Moine et al. (1981).

	Evaporites	Meta-evaporites	Scapolite schists
MgO	high 7-17%*	high 4-20%	medium 5-11%
$Fe_2O_3^{tot}$	3-5%	2-4.5%	3-9%
Li	high 100-300 ppm		low 18-88 ppm
Mg/Al	high 0.8-1.6	0.42-1.68	low 0.14-0.53
Mg/Fe	high 1.5-3.1	1.48-3.81	low 0.39-1.02
K/Al	0.1-0.6	0.17-0.74	0.21-0.54
Na/Al	0.01-0.09	0.02-0.19	0.09-0.28

* - weight %

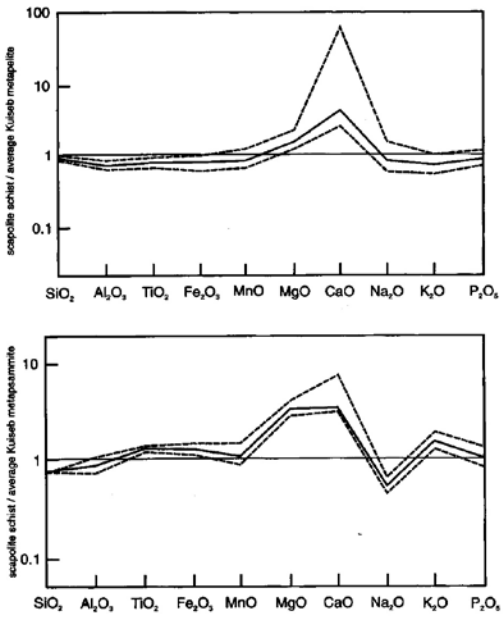

Figure 4: Major element geochemistry of the scapolite schists normalized to average Kuiseb schist compositions after Kukla (1992), dashed lines represent the standard deviation (1 σ).

ence between the scapolite-bearing and scapolite-free parageneses within the Kuiseb Formation (Fig. 4, see also Table 3).

REE geochemistry

In order to obtain additional constraints on the character of the protolith, REE analyses were carried out on four samples of scapolite schist and five samples of scapolite-free Kuiseb metasedimentary rocks (Table 4). Their chondrite-normalized patterns are depicted in figure 5. All samples show light REE (LREE) enrichment and flat heavy REE (HREE) patterns; La_N/Lu_N ranges from 6.1 to 9.2. All show a significant negative Eu-anomaly with Eu/Eu* in the range 0.57 to 0.63 (except for sample AD 93-21 with Eu/Eu* of 0.49). Total REE abundances vary between 159 and 244 ppm in the scapolite schists whilst the scapolite-free meta-sedimentary rocks reveal more uniform contents of 204 to 242 ppm. The following conclusions can be drawn from the REE patterns of the investigated samples:

1) All analysed samples of the Kuiseb Formation show identical REE patterns which means that scapolite-bearing and scapolite-free parageneses have an uniform sedimentary precursor. Virtually the same patterns were found by Hawkesworth *et al.* (1981) and Häussinger *et al.* (1993) for Kuiseb schist samples from different occurrences;
2) Sediments deposited through evaporation would have a distinctly different REE signature because chemical sediments should reflect the composition of the seawater from which they were precipitated. Thus, total concentrations of REE in (meta)-evaporites are expected to be very low (< 10 ppm; Ronov *et al.*, 1974) because of the exceedingly low REE contents of ocean waters (Goldberg *et al.*, 1963; McLennan, 1989). Furthermore, the chondrite-normalized REE patterns of seawater (Goldberg *et al.*, 1963; Høgdahl *et al.*, 1968) usually show a large depletion of Ce and a relative enrichment in HREE (Wedepohl, 1970; Piper, 1974) which is not found in the REE patterns of the Kuiseb schists.
3) The REE patterns of the scapolite-free and scapolite-bearing Kuiseb schists do not deviate significantly from the average of 23 post-Archaean shales (PAAS), reflecting the composition of the upper continental crust (Fig. 6). The Eu/Eu* values are slightly greater than that of PAAS (0.66) and the average La_N/Yb_N ratio of 7.56 suggests somewhat less fractionation than the PAAS value of 9.2.
4) In hydrothermal fluids, the REE are transported as complexes, which are more distinct for each REE than the corresponding ionic compounds (Mineyev, 1963). Thus, the different susceptibilities of the HREE and LREE to complexing, and the different stabilities of the respective complexes, should cause different fractionation within the REE of the scapolite schists -which is not the case. We therefore assume that fluid/rock interaction did not greatly affect the REE contents of the Kuiseb schists;
5) The somewhat lower contents in total REE of the scapolite-bearing samples probably represent a dilution effect caused by the higher density of the scapolite-bearing rocks.

Carbon isotope analyses

STable 1sotope investigations were carried out to shed some light on the origin of the carbon in scapolite and calcite. Evaporation processes strongly affect the isotopic composition of carbon and thus, former evaporitic sediments should be characterized by their heavy $\partial^{13}C$ values (Rothe and Hoefs, 1977). If the scapolitization was caused by externally derived fluids, carbon

Table 3: Bulk rock geochemistry of the Kuiseb metasediments. Rocktypes *pe* = metapelite, *ps* = metapsammite, *scp* = scapolite schist; n.d. = not determined, b.d. = below detection limit, H_2O = LOI-CO_2.

sample numbers: AD93-	1	2A	3	4C	5	6	7	8	9	10	11	12	13	14	15	16	17	18	19	20
wt %	*pe*	*scp*	*scp*	*scp*	*pe*	*pe*	*pe*	*scp*	*scp*	*scp*	*scp*	*scp*	*scp*	*scp*	*ps*	*ps*	*ps*	*scp*	*scp*	*ps*
SiO_2	58.32	52.08	49.61	52.31	56.30	54.19	57.43	50.72	53.75	50.60	54.37	53.22	46.99	68.47	69.25	73.95	73.93	48.94	70.32	74.28
TiO_2	0.72	0.71	0.86	0.70	0.86	0.89	0.80	0.82	0.69	0.78	0.69	0.77	0.63	0.54	0.84	0.57	0.66	1.03	0.55	0.78
Al_2O_3	17.23	16.44	18.68	14.61	18.07	18.83	17.73	18.22	16.21	17.92	15.54	17.33	14.91	11.83	13.54	11.82	11.73	21.15	12.02	11.27
Fe_2O_3	1.88	1.18	2.20	1.50	4.07	4.00	3.50	2.08	0.62	1.41	1.94	2.09	1.60	0.91	1.40	1.18	1.29	4.52	0.89	1.00
FeO	5.5	5.15	5.9	4.2	3.55	4.0	3.85	6.1	6.0	5.9	4.5	5.4	4.3	2.75	4.2	2.3	2.3	4.4	2.3	3.0
MnO	0.06	0.08	0.08	0.09	0.11	0.11	0.08	0.10	0.14	0.10	0.09	0.07	0.09	0.11	0.08	0.05	0.05	0.11	0.07	0.08
MgO	5.44	6.08	7.18	6.74	4.96	5.63	5.24	6.85	5.29	5.83	6.24	5.99	5.04	2.22	2.31	1.52	1.55	5.89	1.44	1.69
CaO	4.23	7.81	6.18	9.33	4.99	5.00	3.05	5.71	7.83	6.94	6.83	6.31	13.16	5.45	1.03	2.67	2.22	5.65	5.76	2.13
Na_2O	1.23	1.54	1.36	1.46	2.01	1.58	1.71	1.39	1.79	2.08	1.28	0.98	0.93	1.96	2.04	2.08	2.15	1.95	1.85	2.45
K_2O	4.25	4.16	4.88	3.38	3.33	3.82	4.51	4.98	3.49	4.27	4.04	4.51	3.53	1.97	3.30	2.20	2.80	4.07	1.61	2.13
P_2O_5	0.17	0.19	0.21	0.19	0.24	0.21	0.21	0.20	0.17	0.20	0.16	0.19	0.17	0.15	0.25	0.27	0.21	0.26	0.16	0.22
H_2O	1.52	1.59	1.71	1.63	1.43	1.57	1.75	1.92	1.82	2.07	1.59	1.55	0.75	1.33	1.61	0.68	0.75	1.43	1.27	0.93
CO_2	n.d.	1.45	0.19	2.35	n.d.	n.d.	n.d.	0.33	1.16	0.73	2.22	0.51	7.24	1.07	n.d.	0.26	n.d.	0.47	0.50	n.d.
Cl	n.d.	0.3	0.4	0.4	n.d.	n.d.	n.d.	0.4	0.4	0.5	0.0	0.2	0.3	0.5	n.d.	b.d.	n.d.	b.d.	0.4	n.d.
total	100.6	98.7	99.5	98.8	99.9	99.8	99.9	99.8	99.4	99.4	99.5	99.1	99.6	99.2	99.9	99.6	99.6	99.9	99.1	100.0
ppm																				
V	137	133	137	100	135	140	115	143	128	133	115	136	113	70	103	72	72	158	69	71
Cr	104	98	96	73	83	86	69	100	106	128	87	120	130	40	72	37	41	102	45	44
Co	37	27	24	19	27	32	21	31	32	21	32	42	29	79	48	56	57	26	45	22
Ni	42	36	42	30	43	47	49	46	34	41	32	38	30	14	31	13	13	53	12	23
Zn	152	82	89	144	121	150	164	77	186	117	140	104	138	54	98	30	53	170	54	75
Ga	29	1	27	25	29	27	28	24	23	27	23	32	26	11	20	17	19	34	21	15
Rb	207	199	240	151	170	194	208	249	182	244	187	214	157	99	130	112	122	204	99	123
Sr	135	210	221	241	173	162	118	191	202	198	155	227	287	200	127	246	247	192	214	187
Y	27	40	38	38	39	44	37	34	33	30	32	29	34	30	36	32	39	48	39	49
Zr	136	142	168	160	173	178	167	155	134	143	129	142	123	181	247	238	336	215	229	436
Nb	15	15	16	14	15	16	18	15	14	14	13	13	11	10	13	10	14	17	12	15
Ba	372	561	567	623	426	517	541	574	500	508	530	736	508	702	701	599	830	523	219	341
Pb	8	<5	<5	6	34	36	24	<5	9	<5	15	9	8	<5	19	<5	<5	37	11	28
Th	8	14	15	7	18	16	14	11	10	11	11	13	11	12	9	12	16	26	15	21
Li	75	75	63	63	56	82	88	63	44	63	88	75	56	25	50	31	37	88	25	31

Table 3: *continued*

sample numbers: AD93-	21	22	23	24	25	26	27	28	29	30	31	32	33	34	35	36	37	38	39	40
wt. %	*scp*	*pe*	*scp*	*pe*	*pe*	*pe*	*ps*	*pe*	*pe*	*pe*	*pe*	*pe*	*pe*	*scp*	*scp*	*scp*	*pe*	*ps*	*pe*	*ps*
SiO2	73.11	56.25	71.19	58.50	62.79	55.57	71.42	46.46	63.77	58.99	56.93	42.50	58.07	46.97	54.10	71.77	57.26	73.11	40.90	69.87
TiO2	0.75	0.75	0.56	0.81	0.96	0.93	0.70	0.96	0.95	0.95	0.78	1.08	0.77	0.95	0.77	0.54	0.84	0.58	1.21	0.70
Al2O3	10.35	20.02	11.07	17.37	15.52	18.85	12.41	21.36	15.72	18.35	17.69	24.38	19.07	19.94	18.13	11.17	18.30	11.72	26.59	13.72
Fe2O3	0.80	1.86	1.64	2.05	1.87	2.37	1.58	1.95	1.85	1.75	1.60	2.83	2.02	8.24	2.19	0.77	1.92	1.92	2.65	1.06
FeO	2.7	6.2	2.2	5.5	5.3	7.1	3.55	7.0	5.1	4.1	5.3	7.1	5.7	1.35	5.3	2.75	6.1	1.9	8.1	3.8
MnO	0.10	0.06	0.06	0.13	0.10	0.11	0.07	0.07	0.08	0.04	0.08	0.07	0.06	0.06	0.08	0.11	0.10	0.14	0.33	0.06
MgO	1.46	3.71	1.78	4.50	3.48	4.03	2.32	6.30	3.81	4.25	5.36	6.79	3.85	7.26	5.49	1.79	3.63	1.95	5.37	2.31
CaO	4.81	1.28	5.59	3.14	1.63	0.64	1.09	6.03	0.58	1.63	5.38	3.17	0.52	3.16	5.94	5.11	2.28	4.32	8.07	2.17
Na2O	2.07	1.81	1.64	1.82	3.73	1.44	2.41	1.08	0.90	2.35	0.92	1.15	0.47	1.22	1.15	1.27	2.05	0.73	0.74	2.96
K2O	1.71	4.99	1.46	4.29	2.74	5.29	2.74	5.11	4.05	3.98	3.99	7.83	5.72	6.90	4.32	1.56	4.37	1.83	4.59	2.33
P2O5	0.20	0.17	0.16	0.18	0.23	0.25	0.18	0.23	0.24	0.21	0.19	0.24	0.18	0.22	0.19	0.15	0.20	0.16	0.23	0.19
H2O	0.83	3.19	1.12	1.67	1.77	3.21	1.35	2.40	2.94	1.95	1.60	3.69	3.38	1.33	2.08	1.01	2.15	1.17	2.25	1.12
CO2	0.36	n.d.	0.12	n.d.	n.d.	n.d.	n.d.	0.41	n.d.	0.12	n.d.	n.d.	n.d.	1.83	0.18	0.82	n.d.	0.72	n.d.	n.d.
Cl	0.2	n.d.	0.3	n.d.	n.d.	n.d.	n.d.	n.d.	n.d.	0.1	n.d.	n.d.	n.d.	0.1	0.3	0.2	n.d.	n.d.	n.d.	n.d.
total	99.5	100.3	98.9	100.0	100.1	99.8	99.8	99.4	100.0	98.7	99.8	100.8	99.8	99.6	100.2	99.0	99.2	100.3	101.0	100.3
ppm																				
V	71	168	69	129	124	153	85	156	115	130	131	141	155	112	111	63	147	71	231	91
Cr	47	108	43	84	90	96	63	119	83	89	98	163	94	100	114	48	97	45	153	60
Co	25	28	35	24	36	36	12	28	22	27	28	26	28	16	29	46	25	36	29	34
Ni	13	49	13	46	41	53	29	43	43	42	34	66	44	43	40	18	46	20	68	26
Zn	54	173	45	155	100	107	73	86	112	43	165	60	127	71	138	92	177	92	238	104
Ga	10	33	16	28	19	24	17	29	24	26	27	37	33	37	37	20	31	14	45	21
Rb	75	241	93	199	147	233	122	299	163	208	183	416	225	365	247	97	228	122	294	140
Sr	258	117	182	253	202	88	138	322	199	344	393	167	57	137	179	187	136	214	249	149
Y	50	40	36	39	45	41	27	38	38	38	25	27	38	34	29	30	44	33	56	40
Zr	461	140	228	166	264	196	209	180	227	219	150	198	143	199	143	203	170	211	245	244
Nb	15	14	11	15	15	14	11	18	16	15	14	19	14	18	16	10	17	12	22	15
Ba	643	585	280	660	263	763	639	732	830	682	812	1236	659	838	366	339	475	359	460	480
Pb	9	48	<5	28	31	8	<5	8	<5	8	<5	<5	<5	10	7	19	39	16	44	21
Th	27	11	11	13	13	15	13	17	12	11	16	<5	13	17	10	9	13	10	26	10
Li	18	69	25	69	37	44	31	75	37	44	50	88	44	69	50	31	69	31	101	37

Table 4: Rare earth element (REE) analyses of selected scapolite-bearing (*) and scapolite-free Kuiseb metasedimentary rocks.

Sample numbers: AD93-	5	8*	9*	13*	21*	24	30	32	35*
(ppm)									
La	41	40	33	31	49	41	41	47	37
Ce	91	82	68	62	94	90	82	99	73
Pr	10	10	8.5	7.4	12	10	9.8	11	9.3
Nd	40	39	33	30	46	40	39	46	35
Sm	8.9	7.6	7.3	6.7	9.6	8.6	7.9	9.7	7.0
Eu	1.5	1.3	1.3	1.1	1.4	1.5	1.3	1.7	1.2
Gd	8.1	7.1	6.5	5.9	9.1	7.8	7.0	8.6	6.4
Tb	1.2	1.2	0.96	0.95	1.4	1.2	1.0	1.3	1.0
Dy	7.5	7.0	6.1	5.8	8.7	7.9	6.2	7.6	6.2
Ho	1.5	1.3	1.1	1.2	1.8	1.6	1.3	1.5	1.1
Er	4.3	3.6	3.3	3.4	4.9	4.9	3.6	4.1	3.2
Tm	0.61	0.51	0.49	0.51	0.7	0.67	0.5	0.57	0.47
Yb	4.1	3.0	3.0	3.3	4.8	4.4	3.5	3.5	2.9
Lu	0.64	0.46	0.48	0.52	0.77	0.68	0.57	0.52	0.44
Eu/Eu*	0.58	0.58	0.63	0.58	0.49	0.61	0.57	0.61	0.59
La_N/Yb_N	6.74	8.97	7.4	6.32	6.87	6.26	7.89	9.04	8.57

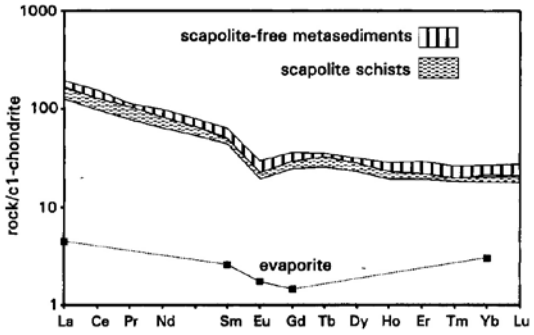

Figure 5: C1-chondrite-normalized REE patterns of the Kuiseb schists.

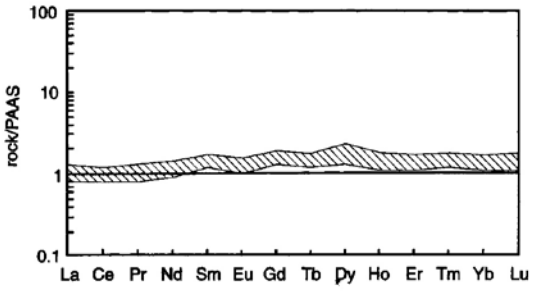

Figure 6: PAAS-normalized REE pattern of the Kuiseb metasedimentary rocks. Values for PAAS-normalization (Post-Archean average Australian shale) are from Nance and Taylor (1976).

should mirror the isotopic characteristics of the fluid phase which interacted with the Kuiseb schists.

The carbon isotopic composition of the investigated scapolite schist samples varies in a narrow range of -8 to -11 ‰ (Table 5, Fig.7) for both scapolite and calcite. A comparison of the data from the scapolite schists in the Khomas Hochland with carbon isotope distributions of the lithosphere and hydrosphere is depicted in Fig.8. In addition, the range of values for the Kuiseb graphite schists and a marble horizon near the Matchless amphibolite in the Khomas Hochland is shown (Kukla, 1992). The average $\Delta_{Scp\text{-}Cc}$ of 0.4 for the scapolite schists of the Kuiseb Formation confirms the assumption of Moecher *et al.* (1994) that fractionation between calcite and scapolite is essentially zero. During evaporation processes an enrichment of the heavier isotope in the remaining sediment occurs. If ocean water with a carbon isotopic composition of around zero is evaporated the resulting $\partial^{13}C$ -values are shifted to higher $^{13}C/^{12}C$ ratios. Thus, evaporation of ocean water is not responsible for the isotopic signature of carbon in the scapolite schists. Another source of CO_2 could be the organic carbon present in the form of graphite schists in the Khomas Hochland, with $\partial^{13}C$ values ranging between -19 and -23 ‰ (Kukla, 1992). Oxidation of this material at lower amphibolite facies temperatures would result in CO_2 with Carbon 9 to 10 ‰ less depleted than the equilibrium graphite (Bottinga, 1969). Thus, the carbon in the scapolites and calcites most likely originated from organic compounds in the sediment pile of the Kuiseb Formation. Derivation of scapolite- and calcite-CO_2 from the marble horizon in the Khomas Hochland by decarbonatization reactions is unlikely. The CO_2-calcite fractionation (Bottinga, 1969) at temperatures of 550-500°C would have required an enrichment of ^{13}C in the scapolite schists by about 2.5-3‰, compared to the marble carbon. We would suggest that this thin marble horizon was invaded by the same CO_2-rich fluid, which caused scapolitization in the siliciclastic rocks.

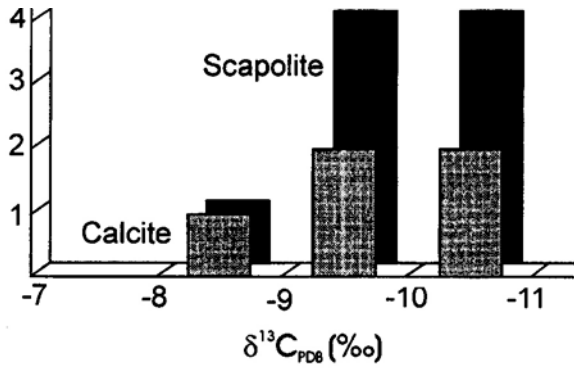

Figure 7: Carbon isotopic composition of CO_2 in sca and calcite of the Kuiseb scapolite schists.

Conclusions

Scapolitization of psammitic and pelitic meta-sedimentary rocks of the Kuiseb Formation gives evidence for the interaction between the metamorphic mineral assemblage and a fluid phase permeating the rocks at the time of metamorphism. On the basis of geochemical data, we exclude an evaporitic origin for the scapolite schists within the Kuiseb Formation. The REE patterns of both scapolite-bearing and scapolite-free Kuiseb schists reveal no evaporitic signature but show a strong similarity to the characteristics of the average upper continental crust represented by PAAS. Furthermore, this interpretation is supported by light $\partial^{13}C$ values of CO_2 in scapolite and calcite, which cannot be the result of evaporation. A conclusive explanation for the light carbon isotopic composition of the scapolite schists in the Kuiseb Formation is derivation from an organic source, probably from graphite within the Kuiseb deposits themselves. This conforms to the uniformity of REE patterns of scapolite-bearing and scapolite-free metasedimentary rocks. If an external fluid input is assumed, changes in the REE contents and fractionation patterns would be expected because chlorine-bearing fluids are favoured complexing ligands for REE. We thus assume a scenario of expulsion of CO_2- and Cl-rich pore fluids from the sediments during progressive deformation leading to the scapolite-forming reaction in the Kuiseb metaturbidites which postdates the D_3 deformation. The fluids concentrated and ascended along shear zones into higher levels of the sediment pile where scapolite formation occurred at the expense of pre-existing plagioclase.

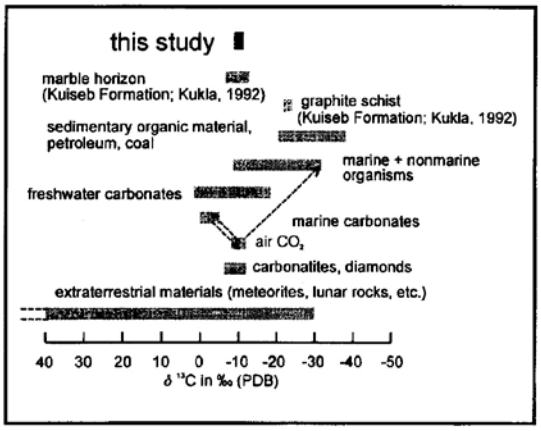

Figure 8: Comparison of $\delta^{13}C$ data from scapolite schists in the Khomas Hochland with carbon isotope distribution of the lithospere and hydrosphere (after Hoefs, 1980). Data for Kuiseb graphite schists and marble in the Khomas Hochland from Kukla (1992).

Table 5: Stable isotope analyses of carbon from scapolite and calcite.

Sample	scapolite $\delta^{13}C_{PDB}$	calcite $\delta^{13}C_{PDB}$
AD93-2	-9.3	-9.2
AD93-3	-9.1	
AD93-4C	-10.2	-10.2
AD93-8	-8.8	
AD93-9	-9.3	-9.1
AD93-13	-10.2	-10.2
AD93-19	-10.6	-8.8
AD93-23	-10.0	
AD93-35	-10.5	

Acknowledgements

This project is funded by the Deutsche Forschungsgesellschaft. Thanks are due to Jorg Erzinger at the GeoForschungsZentrum Potsdam for usefull discussions during sample preparation and REE analyses. We highly appreciate the constructive critisism of this manuscript by Hartwig Frimmel, University of Cape Town, and an anonymous reviewer. The final version benefited much from the review of Nigel Cook which was particularly helpful in improving the English.

References

Behr, H.J., Ahrendt, H., Porada, H., Röhrs, J. and Weber, K. 1983. Upper Proterozoic playa and sabkha deposits in the Damara orogen, SWA/Namibia. *In*: R. McG. Miller (ed.), *Evolution of the Damara Orogen of SouthWest Africa/Namibia*, Spec. Publ. geol. Soc. S. Afr., **11**, 1-20.

Bottinga, Y. 1969. Carbon isotope fractionation between graphite, diamond and carbon dioxide. *Earth & Planet. Sci. Lett.*, **5**, 301-307.

Bühn, B., Häussinger, H., Kramm, U., Kukla, C., Kukla, P.A. and Stanistreet, I.G. 1994. Tectonometamorphic patterns developed during Pan-African continental collision in the Damara Inland Belt, Namibia. *Chem. Erde*, **54**, 329-354.

Evensen, N.M., Hamilton, P.J. and O'Nions, R.K. 1978. Rare-earth abundances in chondri tic meteo-rites. *Geochim. Cosmochim. Acta*, **42**, 1199-1212.

Goldberg, E.D., Koide, M., Schmitt, R.A. and Smith, R.H. 1963. Rare-earth distributions in the marine environment. *J. Geophys. Res.*, **68**, 4209-4217.

Gómez-Pugnaire, M.T., Franz, G. and Sánchez-Vizcaino, V.L. 1994. Retrograde formation of NaCl-scapolite in high pressure metaevaporites from the Cordillera Béticas (Spain). *Contrib. Mineral. Petrol.*, **116**, 448-461.

Häussinger, H., Okrusch, M. and Scheepers, D. 1993. Geochemistry of premetamorphic hydrothennal alteration of metasedimentary rocks associated with the Gorob Massive Sulfide Prospect, Damara Oro-

gen, Namibia. *Econ. Geol.*, **88**, 72-90.

Hartmann, O., Hoffer, E. and Haack, U. 1983. Regional metamorphism in the Damara Orogen: interaction of crustal motion and heat transfer. *In*: R McG. Miller (ed.), *Evolution of the Damara Orogen of SouthWest Africa/Namibia*. Spec. Publ. geol. Soc. S. Afr., **11**, 233-241.

Hawkesworth, C.J., Kramers, J.D. and Miller, RMcG. 1981. Old model Nd ages in Namibian Pan-African rocks. *Nature,* **289**, 278-282.

Hoefs, J. 1980. *STable 1sotope geochemistry*. Springer- Verlag, Berlin, 208 pp.

Høgdahl, O.T., Melson, S. and Bowen, V.T. 1968. Neutron activation analysis of lanthanide elements in seawater. *In*: Baker, RA (ed.), *Trace inorganics in water*. Adv. Chem. Ser., **73**, 308-325.

Kukla, C. 1993. Strontium isotope heterogeneieties in amphibolite facies, banded metasediments - A case study from the Late Proterozoic Kuiseb Formation of the southern Damara Orogen, central Namibia. *Mem. geol. Surv. Namibia*, **15**, 139 pp.

Kukla, P.A. 1990. Unususal scapolitization of Late Proterozoic deep-sea fan sequences in an amphibolite-grade metamorphic terrain, Damara Orogen, Central Namibia. *Eur. J. Mineral. Beih.*, **2**, 145.

Kukla, P.A. 1992. Tectonics and sedimentation of a late Proterozoic Damaran convergent continental margin, Khomas Hochland, Central Namibia. *Mem. geol. Surv. Namibia*, **12**, 95pp.

Kukla, P.A and Stanistreet, I.G. 1991. Record of the Damaran Khomas Hochland accretionary prism in Central Namibia: refutation of an 'ensialic' origin of a Late Proterozoic orogenic belt. *Geology,* **19**, 473-476.

McLennan, S.M. 1989. Rare earth elements in sedimentary rocks: influence of provenance and sedimentary processes. *In*: Lipin, B.R. and McKay, G.A (eds.) *Geochemistry and mineralogy of rare earth elements*. Reviews in Mineralogy, **21**, 169-200.

McLennan, S.M., Taylor, S.R, McCulloch, M.T. and Maynard, J.B. 1990. Geochemical and Sr-Nd isotopic composition of deep-sea turbidites: crustal evolution and plate tectonic association. *Geochim. Cosmochim. Acta*, **54**, 2015-2050.

Mineyev, D.A. 1963. Geochemical differentiation of the rare-earth elements. *Geochemistry,* **12**, 1129-1149.

Moecher, D.P., Valley, J.W. and Essene, E.J. 1994. Extraction and carbon isotope analysis of CO_2 from scapolite in deep crustal granulites and xenoliths. *Geochim. Cosmochim. Acta*, **58**, 959-967.

Moine, B., Sauvan, P. and Jarousse, J. 1981. Geochemistry of evaporite-bearing series, a tentative guide for the identification of meta-evaporites. *Contrib. Mineral. Petrol.*, **76**, 401-412.

Mora, C.L and Valley, J.W. 1989. Halogen-rich scapolite and biotite: implications for metamorphic fluid - rock interaction. *Am. Mineral.*, **74**, 721-737.

Nance, W.B. and Taylor, S.R 1976. Rare earth element patterns and crustal evolution - L Australian post-Archaean sedimentary rocks. *Geochim. Cosmochim. Acta*, **40**, 1539-1551.

Oliver, N.H.S., Wall, V.J. and Cartwright, I. 1992. Internal control of fluid compositions in amphibolite-facies scapolitic calc-silicates, Mary Kathleen, Australia. *Contrib. Mineral. Petrol.*, **111**, 94-112.

Orville, P.M. 1975. Stability of scapolite in the system Ab-An-NaCl-$CaCO_3$ at 4 kb and 750°C. *Geochim. Cosmochim. Acta*, **39**, 1091-1105.

Piper, D.Z. 1974. Rare earth elements in ferromanganese nodules and other marine phases. *Geochim. Cosmochim. Acta*., **52**, 1373-1382.

Ronov, A.B., Balashov, Yu.A, Girln, Yu.P., Bratishko, R.Kh. and Kazakov, G.A. 1974. Regularities ofrare-earth element distribution in the sedimentary shell and in the crust of the earth. *Sedimentology,* **21**, 171-193.

Rothe, P. and Hoefs, J. 1977. Isotopengeochemische Untersuchungen an Karbonaten der Ries-See-Sedimente der Forschungsbohrung Nördlingen. *Geol. Bavaria*, **75**, 59-66.

Shaw, D.M. 1960. The geochemistry of scapolite. Part L previous work and mineralogy. *J. Petrol.*, **1**, 218-260.

Wedepohl, 1970. *Handbook of Geochemistry, Vol. 11/5, Elements La (57) to U (92)*. Springer-Verlag, Berlin.

Zuleger, E. and Erzinger, J. 1988. Determination of the REE and Y in silicate materials with ICP-AES. *Fresenius Z. Anal. Chem*., **332**, 140-143.